Nuclear Instruments and Methods in Physics Research A 755 (2014) 28–31

Contents lists available at ScienceDirect

Nuclear Instruments and Methods in Physics Research A

journal homepage: www.elsevier.com/locate/nima

Reconstruction of finer voxel grid transmission images in Tomographic Gamma Scanning

Ke Wang [a,b], Zheng Li [a,b,*], Wei Feng [a,b]

[a] Key Laboratory of Particle & Radiation Imaging (Tsinghua University), Ministry of Education, China
[b] Department of Engineering Physics, Tsinghua University, China

ARTICLE INFO

Article history:
Received 3 March 2014
Received in revised form
15 April 2014
Accepted 17 April 2014
Available online 28 April 2014

Keywords:
Tomographic Gamma Scanning
Image reconstruction
Total variation
Attenuation process

ABSTRACT

Tomographic Gamma Scanning (TGS) is a technique used to assay the nuclide distribution and radioactivity in nuclear waste drums. Limited to few transmission measurements, the drum is divided into large voxels and thus leads to the inhomogeneity of the voxels and negatively affects the results. A new algorithm is presented to reconstruct finer voxel grid transmission images with the same number of measurements. The small voxel size decreases the effect of the inhomogeneity and makes the result more accurate. The algorithm employs total variation minimization and precisely describes the attenuation process. The influences of the different scan modes are discussed with Monte Carlo simulations. Experiments are performed to verify the effectiveness of our method.

1. Introduction

Before nuclear waste drums are disposed, detecting nuclide distribution and radioactivity is necessary to meet safety requirements. Tomographic Gamma Scanning (TGS) is one of the most advanced nondestructive assay techniques. Both the locations and quantities of radioisotopes can be accurately measured. The first TGS system was developed in the Los Alamos National Laboratory in the early 1990s [1]. A similar device called A&PCT was also manufactured by the Lawrence Livermore National Laboratory during the same period [2]. Different devices have been established, and much research has investigated TGS ever since [3–5]. Although commercial TGS systems are available [6,7], the TGS technique still needs improvements.

TGS detections need to scan the drum twice, one for transmission measurement with an external isotopic source and the other for emission measurement without such a source. The emission image displays the distribution of the radionuclides in the drum, whereas the transmission image shows the attenuation coefficient matrix. The latter is used for attenuation correction when reconstructing the emission image. Typically, the number of projections is quite small given the limited scanning time. As a result, the number of voxels is also limited given the ordinary image reconstruction discipline. This number also increases the voxel size, which is close to the size of the collimator aperture. Each voxel is assumed to be uniform in image reconstructions. However, this usually does not apply to real drums because of the large voxel size. The heterogeneity of transmission image voxels influences the accuracy of attenuation correction factors. Although decreasing the voxel size improves heterogeneity, it increases scanning time to obtain more projections to reconstruct the images.

In medical image reconstruction, compressed sensing theory is applied when projections are sparsely sampled. This theory asserts that certain images can be recovered from far fewer samples or measurements than is required by Nyquist sampling theory.[8] Among various compressed sensing methods, total variation (TV) minimization [9] is one of the most commonly used methods. For TGS, obtaining finer voxel grid images with the TV minimization method is possible when the number of measurements remains the same. However, simply applying the TV minimization method is insufficient. When the detector area or the collimator aperture size is much larger than the voxel size, a more accurate description of the attenuation process is needed.

In this paper, a new algorithm employing the TV minimization method is presented for finer voxel grid transmission images with the same number of measurements. The scan modes of TGS for our algorithm are also discussed with Monte Carlo simulations. A simple TGS prototype is constructed to confirm the effectiveness of the algorithm.

2. Methods

2.1. Transmission scan

According to Beer's law, the transmission scan of a specific energy E is described as follows:

$$N_i = N_0 \exp(-\sum_j t_{ij}\mu_j), \quad (1)$$

* Corresponding author. Tel.: +86 135 0121 1903.
E-mail address: lizheng@mail.tsinghua.edu.cn (Z. Li).

http://dx.doi.org/10.1016/j.nima.2014.04.046
0168-9002/

where N_0 is the count rate of energy E attenuated by air only, N_i is the count rate in the ith transmission scan, t_{ij} is the trace length of the jth voxel along the ray from the external isotopic source to the detector, and μ_j is the attenuation coefficient of the jth voxel to be solved. Each voxel is supposed to be uniform in the transmission scan.

Eq. (1) can be converted into a linear form

$$g_i = \sum_j t_{ij}\mu_j, \tag{2}$$

where $g_i = -\ln(N_i/N_0)$. Among the various algorithms that can be used to solve Eq. (2), the Algebra Reconstruction Technique (ART) algorithm is the most preferred in the transmission image reconstruction of TGS

$$\mathbf{f}^{(r+1)} = \mathbf{f}^{(r)} + \frac{g_i - \mathbf{H}_i\mathbf{f}^{(r)}}{\|\mathbf{H}_i\|^2}\mathbf{H}_i^T, \tag{3}$$

where $\mathbf{f}=\{\mu_j\}$, $\mathbf{H}_i=\{t_{ij}\}|_{j=1:J}$, and r is the iteration number.

2.2. Emission scan

The emission scan measures the gamma-ray counts from the nuclear waste drum. The ray sum of a specific energy E in the ith measurement is defined as follows:

$$p_i = \sum_j \varepsilon_{ij} a_{ij} s_j, \tag{4}$$

where p_i is the count rate of the ith measurement of energy E and s_j is the activity of the radioactive source in the jth voxel. Considering that the branch ratio of a specific energy is a constant, it is ignored in Eq. (4) and is processed after the emission reconstruction. ε_{ij} is the detection efficiency if a radioactive source is placed in the jth voxel without any attenuation. a_{ij} is the attenuation correction factor, described as follows:

$$a_{ij} = \prod_m \exp(-t_{ijm}\mu_m), \tag{5}$$

where μ_m is the attenuation coefficient of the mth transmission voxel that can be obtained from the transmission scan result and t_{ijm} is the length in voxel m along the ray connecting the emission voxel j and the detector.

The distribution of the activity can be obtained by solving Eq. (4). The Maximum-Likelihood Expectation–Maximization algorithm is proven to be effective [10]

$$s_j^{(k+1)} = \frac{s_j^{(k)}}{\sum_i F_{ij}} \sum_i F_{ij} \frac{p_i}{\sum_l F_{il} s_l^{(k)}}, \tag{6}$$

where $F_{ij}=\varepsilon_{ij}\, a_{ij}$ and k is the iterative number.

2.3. Reconstruction of finer voxel grid transmission images

The TV minimization method usually works together with iterative image reconstruction algorithms, such as ART. During ART iteration processes, the total variation of the transmission image is minimized with the gradient descent method [9]

$$\mathbf{f}^{(k,l_{TV}+1)} = \mathbf{f}^{(k,l_{TV})} - \alpha d^{(k)} \frac{\mathbf{v}}{\|\mathbf{v}\|_2}, \tag{7}$$

where $\mathbf{f}$ is the image to be reconstructed, k is the iterative number of ART, l_{TV} is the iterative number of TV minimization during the kth ART iteration, α is the relaxation index, and $d^{(k)}$ and each element of $\mathbf{v}$ are described as follows:

$$d^{(k)} = \|\mathbf{f}^{(k,0)} - \mathbf{f}^{(k-1,N_{TV}-1)}\|_2, \tag{8}$$

$$v_{s,t} = \frac{\partial \|\vec{f}\|_{TV}}{\partial f_{s,t}} \approx \frac{2f_{s,t} - f_{s-1,t} - f_{s,t-1}}{\sqrt{\varepsilon + (f_{s,t} - f_{s-1,t})^2 + (f_{s,t} - f_{s,t-1})^2}}$$
$$- \frac{f_{s+1,t} - f_{s,t}}{\sqrt{\varepsilon + (f_{s+1,t} - f_{s,t})^2 + (f_{s+1,t} - f_{s+1,t-1})^2}},$$
$$- \frac{f_{s,t+1} - f_{s,t}}{\sqrt{\varepsilon + (f_{s,t+1} - f_{s,t})^2 + (f_{s,t+1} - f_{s-1,t+1})^2}} \tag{9}$$

where N_{TV} is the iterations of TV minimization during each ART iteration and ε is a small positive number. This equation is the so-called ART–TV algorithm widely used in medical image reconstruction.

However, directly applying the ART–TV algorithm to the transmission reconstruction of TGS for finer voxel grid transmission images does not work because the detector is much larger than the voxels. When the voxels become smaller, Eq. (1) cannot describe the attenuation process well. Some of the small voxels are not passed through by the rays, although they contribute to the attenuation. If the middle ray connecting the source and the detector center is the only ray considered, the dark voxels are not calculated in this transmission measurement, although they have contributions to the system (Fig. 1).

When the voxel is much smaller than the detector, the transmission measurements can be described by a more accurate model as follows [11]:

$$N_i = \sum_{n=1}^{N_0} \exp(-\sum_{j=1}^{J} t_{ijn}\mu_j), \tag{10}$$

where N_0 is the number of gamma rays which emit from the external source and can be detected. In Eq. (10), the detection efficiency of each gamma ray is assumed to be the same. Although Eq. (10) gives a more accurate description, solving such nonlinear equations is difficult.

On the other hand, if the attenuation coefficient of a voxel is known, the relative length of this voxel is available

$$t_{ij}^* = -\frac{1}{\mu_j}\ln\left(\frac{1}{N_0}\sum_{n=1}^{N_0}\exp(-t_{ijn}\mu_j)\right). \tag{11}$$

Thus, we can use an iteration process to approach the true attenuation coefficient proposed by Zhang et al.[11]. The detector front-face is divided into N_0 pixels to calculate t_{ijn}, and each pixel is small enough compared with the voxel size. t_{ijn} is the trace length of the jth voxel along the ray connecting the source and the nth detector pixel.

The steps of the algorithm are as follows:

(1) An initial guess $\mu_j^{(0)}$ in Eq. (2) is obtained with the ART–TV algorithm. The initial $t_{ij}^{*(0)}$ in Eq. (2) is as follows:

$$t_{ij}^{*(0)} = \frac{1}{N_0}\sum_{n=1}^{N_0} t_{ijn}. \tag{12}$$

(2) $t_{ij}^{*(k)}$ is calculated by substituting $\mu_j^{(k-1)}$ for μ_j in Eq. (11).
(3) $t_{ij}^{*(k)}$ is substituted in Eq. (2), and $\mu_j^{(k)}$ is solved with ART–TV.

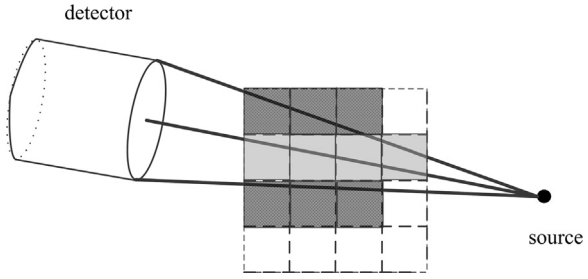

Fig. 1. Differences between signal ray and cone beam.

(4) If $\frac{\|\mathbf{f}^{(k)}-\mathbf{f}^{(k-1)}\|}{\|\mathbf{f}^{(k-1)}\|}<\varepsilon$, where $\mathbf{f}^{(k)}=\{\mu_j^{(k)}\}$, or $k\geq K$, the iteration ends. If not, then the algorithm continues from step 2.

3. Simulations and experiments

3.1. Simulations

Monte Carlo simulations are performed to examine the effectiveness of the different scan modes when our new algorithm is applied. The simulation model is shown in Fig. 2. The size of this model is similar to that of a real TGS device. We use two different scan modes in the transmission scan. In the first scan mode, the object translates 10 times over 56 cm and rotates 20 times over 180°. In the second scan mode, it translates 20 times over 56 cm and rotates 10 times over 180°. Scan mode 1 means a denser sampling in the rotation and scan mode 2 means a denser sampling in the translation. The step number cannot be less than 10, otherwise some voxels may not be scanned. If the rotation number is less than 10, it may cause problems when reconstructing images. Although the scan mode used in commercial systems (the drum is scanned from its edge to center and back to the edge) may work better, it is not supported by our experimental prototype at the moment. The scan mode of continuous movement is the same. Only the rotate–translate scan mode described above are available at present.

The results of the two scan modes are shown in Fig. 3. A comparison of Fig. 3(b) and (c) shows that the latter is clearly better than the former. The edges of the objects are clearer, and the consistency (the same material should have the same value) is better in Fig. 3(c). A denser sampling in the translation enhances the edge and improves the transmission image. Thus, we use scan mode 2 in the transmission scan of the following experiments.

3.2. Experimental setup

The voxel size of a typical TGS device is approximately 6 cm. Approximately 16 or 17 layers are present in a 208 L waste drum, and each layer is divided into 10×10 voxels. Given the limitations in the experimental conditions, the prototype used here is smaller than the real TGS. The maximum diameter of the object that can be scanned is 20 cm. The voxel size is 2 cm if each layer is divided into 10×10 voxels. The square aperture size of the collimator is also 2 cm. The TGS prototype is quite similar to that shown in Fig. 2, and the sizes decrease accordingly. For simplicity, only one layer is scanned in the experiments.

Other than the transmission scan, the emission scan is performed to verify the improvements of the attenuation correction factors from the new transmission reconstruction algorithm. The

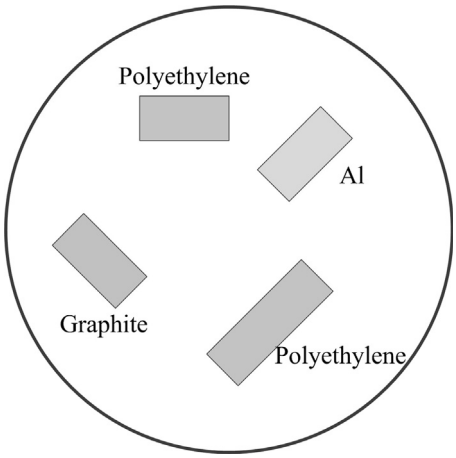

Fig. 4. Experimental models. The circle represents the edge of the objective table.

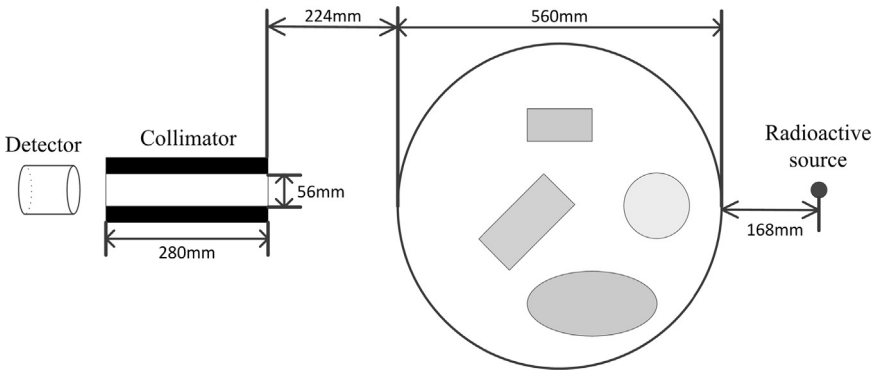

Fig. 2. Simulation model.

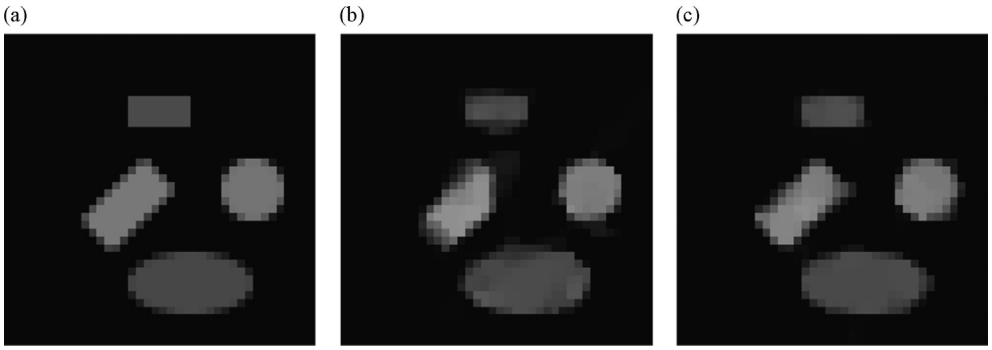

Fig. 3. Simulation results. The gray scale window is [0 0.3], and each image size is 40×40.(a) Reference image. (b) Results of scan mode 1. (c) Results of scan mode 2.

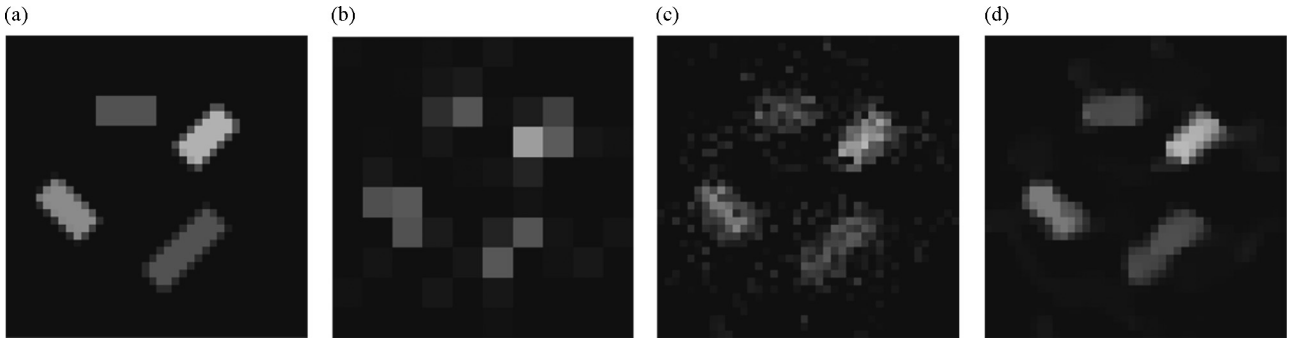

Fig. 5. Reconstruction results. The gray scale window is [0 0.3]. (a) Reference image, 40×40 pixels. (b) Reconstructed with ART, 10×10 pixels. (c) Reconstructed with ART, 40×40 pixels. (d) Reconstructed with our algorithm, 40×40 pixels.

detection efficiency matrix is obtained from the Monte Carlo simulations. To exclude the interference of the error from the detection efficiency, a special emission scan is performed when no attenuation material exists and the radioactive source is at the same place as the normal emission scans. The reconstruction result of this emission scan is taken as the reference activity.

3.3. Experimental results

The materials used in the experiments are shown in Fig. 4. All the objects in Fig. 4 are cylindrical. We use a ^{137}Cs as the external transmission source. An annular ^{137}Cs is also placed in the center of the models as the emission source.

The reconstruction results are shown in Fig. 5. Fig. 5(a) is the reference image. The attenuation coefficients of the materials in Fig. 5(a) are obtained from the additional attenuation experiments. Fig. 5(b), whose size is 10×10 pixels, is reconstructed with ART. A 10×10 pixel image cannot describe the model in Fig. 4 accurately, resulting in inaccuracies in both values and shapes. Fig. 5(c) also shows the reconstructed result with ART. This result is an ill-posed problem with 200 measurements and 1600 unknowns. Fig. 5(c) shows that reconstructing finer voxel grid transmission images with traditional algorithms is infeasible. Fig. 5(d) is the result of our algorithm. Both the shape and consistency of Fig. 5(d) are much better than those of Fig. 5(b). Comparing Fig. 5(d) with Fig. 3(c), the former is nearly as good as the latter which is from the simulated data.

The mean square errors (MSEs) of Fig. 5(b) and (d) are shown in Table 1. The MSE of Fig. 5(b) is calculated by dividing it into a 40×40 pixel image, as the size of the reference image is 40×40. Table 1 also displays the total activities of the emission reconstruction results and their relative errors, whose attenuation factors are obtained from Fig. 5(b), (d) and (a). The reference activity is from the reconstruction of the emission scan without any attenuation. The activity error of Fig. 5(d) is only about half of Fig. 5(b) and is quite close to that of Fig. 5(a).

Table 1
MSE and total activity.

	MSE	Activity* (μCi)	Error of activity/%
Fig. 5(b)	4.62×10^{-4}	4.4454	0.59
Fig. 5(d)	3.08×10^{-4}	4.4073	−0.27
Fig. 5(a)	0	4.4079	−0.26

* The reference activity is 4.4194 μCi.

4. Conclusion

This study proposes an algorithm that employs TV minimization to reconstruct finer voxel grid transmission images of TGS. We use an accurate description of the attenuation process compared with the conventional transmission reconstruction in the algorithm. Monte Carlo simulations show that dense sampling in the translation motion yields the desired result when the total sample number remains the same. Experiments are performed to verify the effectiveness of our algorithm. The experimental results show that our finer voxel grid transmission reconstruction methods generate accurate attenuation correction factors compared with conventional methods that employ ART.

Acknowledgment

This work is supported by the National Natural Science Foundation of China (No. 11175101).

References

[1] R.J. Estep, T.H. Prettyman, Nuclear Science and Engineering 118 (1994) 145.
[2] G. Roberson, H. Martz, D. Decman, et al., Characterization of waste drums using nonintrusive active and passive computed tomography, UCRL-JC-118317, Lawrence Livermore National Laboratory, 1994.
[3] G. Roberson, H. Martz, D. Camp, et al., Preliminary A&PCT multiple detector design, upgrade of a single HPGe detector A&PCT system to multiple detectors, UCRL-ID-128052, Lawrence Livermore National Laboratory, 1997.
[4] C. Robert-Coutant, V. Moulin, R. Sauze, et al., Nuclear Instruments and Methods A 422 (1999) 949.
[5] W. Gu, C. Liu, N. Qian, et al., Annals of Nuclear Energy 58 (2013) 113.
[6] R. Venkataraman, S. Croft, M. Villani, et al., The next generation tomographic gamma scanner, in: Proceedings of the 27th Annual Meeting ESARDA (European Safeguards Research and Development Association) Symposium on Safeguards and Nuclear Material Management, London, England, 2005.
[7] R. Venkataraman, M. Villani, S. Croft, et al., Nuclear Instruments and Methods A 579 (2007) 375.
[8] E.J. Candès, M.B. Wakin, IEEE Signal Processing Magazine 25 (2008) 21.
[9] E.Y. Sidky, C.M. Kao, X. Pan, Journal of X-ray Science and Technology 14 (2006) 119.
[10] T.H. Prettyman, R.A. Cole, R.J. Estep, et al., Nuclear Instruments and Methods A 356 (1995) 470.
[11] Q. Zhang, W. Hui, F. Li, et al., Researches on the key technologies for Tomographic Gamma Scanning, in: Proceedings of the 18th International Conference on Nuclear Engineering, ICONE18, Xi'an, China, 2010.